Distribution of Ganglioside GM1 in L-α-Dipalmitoylphosphatidylcholine/Cholesterol Monolayers: A Model for Lipid Rafts[1]

Chunbo Yuan and Linda J. Johnston
Steacie Institute for Molecular Sciences, National Research Council of Canada, Ottawa, Ontario K1A 0R6, Canada

ABSTRACT The distribution of low concentrations of ganglioside GM1 in L-α-dipalmitoylphosphatidylcholine (DPPC) and DPPC/cholesterol monolayers supported on mica has been studied using atomic force microscopy (AFM). The monolayers studied correspond to a pure gel phase and a mixture of liquid-expanded (LE) and liquid-condensed (LC) phases for DPPC and to a single homogeneous liquid-ordered phase for 2:1 DPPC/cholesterol. The addition of 2.5–5% GM1 to phase-separated DPPC monolayers resulted in small round ganglioside-rich microdomains in the center and at the edges of the LC domains. Higher amounts of GM1 (10%) give numerous filaments in the center of the LC domains and larger patches at the edges. A gel phase DPPC monolayer containing GM1 showed large domains containing a network of GM1-rich filaments. The addition of GM1 to a liquid-ordered 2:1 DPPC/cholesterol monolayer gives small, round domains that vary in size from 50 to 150 nm for a range of surface pressures. Larger amounts of GM1 lead to coalescence of the small, round domains to give longer filaments that cover 30–40% of the monolayer surface for 10 mol % GM1. The results indicate that biologically relevant GM1 concentrations lead to submicron-sized domains in a cholesterol-rich liquid-ordered phase that is analogous to that found in detergent-insoluble membrane fractions, and are thought to be important in membrane microdomains or rafts. This demonstrates that AFM studies of model monolayers and bilayers provide a powerful method for the direct detection of microdomains that are too small for study with most other techniques.

INTRODUCTION

There is increasing evidence that lateral organization of lipids in cellular membranes plays an important role in a diverse range of processes, such as membrane trafficking and signaling. Simons and Ikonen (1997) have recently proposed a model in which preferential packing of sphingolipids and cholesterol results in microdomains or lipid rafts to which specific membrane proteins are attached. In this model, glycosphingolipids associate laterally with one another, probably through weak carbohydrate interactions. The large size of the (glyco)sphingolipid headgroups relative to their predominantly saturated lipid hydrocarbon chains leads to voids that are filled by cholesterol spacers. A variety of membrane proteins and glycosylphosphatidylinositol (GPI)-anchored proteins are thought to localize in lipid rafts, leading to their potential involvement in protein sorting and signaling pathways. Although phase separation in model membranes has been extensively studied, much of the evidence for the existence of microdomains in biological membranes has come from the extraction and characterization of detergent-insoluble membrane fractions that are rich in sphingolipids and cholesterol (Brown and London, 1998a, b). These domains are believed to exist in a liquid-ordered phase that has properties intermediate between those of liquid-disordered and gel phases. Despite the increasing recognition of the importance of lateral membrane organization, the detection of lipid domains in vivo remains a significant challenge (Jacobson and Dietrich, 1999). Some of the most convincing evidence for in vivo raft formation comes from the recent findings that GPI-anchored proteins are organized in submicron domains at the cell surface (Friedrichson and Kurzchalia, 1998; Varma and Mayor, 1998). One of the difficulties in many studies is the fact that the formation and/or aggregation of the lipid microdomains may be facilitated by cross-linking with the probes that are used for their detection (Brown and London, 1998b; Harder et al., 1998).

The use of phospholipid mono and bilayers has proven invaluable in studying lipid properties and should provide an equally attractive method for studying raft formation in model systems. We have used atomic force microscopy (AFM) to study domain formation induced by ganglioside GM1 in L-α-dipalmitoylphosphatidylcholine (DPPC)/cholesterol monolayers as a model system for raft formation. Gangliosides are glycosphingolipids containing sialic acid that are primarily found in the outer leaflet of plasma membranes in vertebrate tissue. Although a minor component in most cells, they constitute ~5–10% of the total lipid mass in nerve cells (Derry and Wolfe, 1967). Because they are located primarily in the outer leaflet of membranes, the external surfaces of some plasma membranes, such as glial cells, may contain 10–20 mol % gangliosides. Ganglioside GM1, which contains four neutral sugars and a negatively charged sialic acid, has been extensively investigated; it has been previously used as a raft marker (Harder et al., 1998) because it is a common ganglioside in many plasma membranes and the natural receptor for the cholera toxin B subunit, thus facilitating its direct detection.

Received for publication 20 April 2000 and in final form 24 July 2000.

Address reprint requests to Linda J. Johnston, Steacie Institute for Molecular Sciences, National Research Council Canada, Ottawa, Ontario K1A 0R6, Canada. Tel.: 613-990-0973; Fax: 613-952-0068; E-mail: Linda.Johnston@nrc.ca.

[1] Issued as NRCC 43848.

0006-3495/00/11/2768/14 $2.00

The organization of gangliosides in model membranes has been extensively investigated with various methods, such as freeze-etch electron microscopy (Mehlhorn et al., 1986; Rock et al., 1991; Thompson et al., 1985), differential scanning calorimetry (DSC) (Bach et al., 1982; Ferraretto et al., 1997; Holopainen et al., 1997; Terzaghi et al., 1993), electron spin resonance (ESR; Delmelle et al., 1980; Sharom and Grant, 1978), and x-ray diffraction (McIntosh and Simon, 1994). The results of these studies do not lead to a consistent picture of the distribution of gangliosides in model membranes. DSC studies of mixtures of PC with small quantities of ganglioside generally indicate that gross phase separations do not occur over broad temperature ranges, suggesting that the ganglioside is completely miscible with PC in the liquid crystalline state (Thompson et al., 1985). By contrast, the direct visualization of GM1 distribution (7 mol %) in 1:1 DPPC/dielaidoyl phosphatidylcholine (DEPC) bilayers by freeze-etch electron microscopy using lectin (Peters and Grant, 1984) and agglutinin (Peters et al., 1984) as ganglioside labels shows that the ganglioside partitions in both gel and liquid crystalline regions and self-associates in clusters. However, Thompson et al. (1985) used freeze-etch electron microscopy to assess the distribution of GM1 in 1-palmitoyl-2-elaidoyl phosphatidylcholine (PEPC) bilayers after labeling with cholera toxin and ferritin-labeled cholera toxin. They found that at low concentration ($<$5 mol %) GM1 molecules are randomly distributed in the liquid crystalline state of the bilayer. They also concluded that GM1 molecules are evenly distributed in dimyristoyl phosphatidylcholine (DMPC) bilayers in both gel and liquid crystalline states. In addition, the study of the distribution of GM1 in 1:1 DPPC/DEPC bilayers (Rock et al., 1991) with cholera toxin-labeled GM1 shows that at low concentration ($<$1%) GM1 is preferentially incorporated in the gel phase. Delmelle et al. (1980) used spin-labeled gangliosides to approach the problem of ganglioside clustering of DPPC bilayers by ESR and concluded that GM1 is randomly distributed in the liquid crystalline state and clustered in the gel state. The contrasting conclusions from the various studies suggest that both the type of model bilayer system and the method used may play key roles in assessing ganglioside distributions.

AFM provides a useful alternative for studies of morphology and phase separation in supported monolayers and bilayers and has the advantage of allowing for direct detection of submicron and even nanometer-scale domains under physiological conditions in aqueous solution (Chi et al., 1993; Dufrene et al., 1997; Hollars and Dunn, 1997, 1998; Mou et al., 1995; Overney et al., 1992; Rinia et al., 1999; Yang et al., 1995). The distribution of GM1 in two-component phase-separated dioleoylphosphatidylcholine (DOPC)/DPPC monolayers on mica has been elegantly investigated by Vie et al. (1998). Their results provide convincing evidence that GM1 is heterogeneously distributed in the condensed DPPC phase, at least at low concentrations. Recent fluorescence microscopy experiments also demonstrate that GM1 induces heterogeneity in DPPC monolayers (Hwang et al., 1995). Nevertheless, these results are in contrast to the uniform distribution of GM1 that has been observed by AFM studies of both fluid and gel phase bilayers, using cholera toxin as a probe (Mou et al., 1995). In this paper, we report results of AFM studies of the distribution of GM1 in pure DPPC and mixed DPPC/cholesterol monolayers prepared by Langmuir-Blodgett transfer. Our results demonstrate that GM1 localizes in the condensed phase in DPPC monolayers containing a mixture of liquid-expanded (LE) and liquid-condensed (LC) phases and is heterogeneously distributed within this phase. The incorporation of GM1 in DPPC/cholesterol monolayers provides striking evidence for heterogeneity, with the observation of small GM1-rich microdomains that we believe are relevant to mechanisms of raft formation in membranes.

MATERIALS AND METHODS

DPPC (Avanti Polar Lipids, Alabaster, AL), monosialoganglioside-GM1 (Sigma, St. Louis, MO, bovine brain extract), and cholesterol (Sigma) were used as received. DPPC and cholesterol (1 mg/ml) were dissolved in chloroform. GM1 was dissolved in chloroform/methanol (v/v, 80:20) at a concentration of 0.4 mg/ml. DPPC/GM1 mixtures were prepared in three molar ratios (2.5%, 5%, and 10% GM1); DPPC/cholesterol/GM1 mixtures were prepared in molar ratios of 60:30:10 and 68:30:2.

Monolayers of DPPC and DPPC/GM1 mixtures were prepared on a Langmuir-Blodgett trough (NIMA 611, Coventry, UK) using Milli-Q water as the subphase. The sample solutions (DPPC in chloroform, and GM1 in chloroform/methanol, 80:20 v/v) were spread on the subphase surface; after solvent evaporation (10 min) the monolayers were compressed at 50 cm^2/min to the required surface pressure. The surface pressure was measured with a precision of 0.1 mN/m using a Wilhelmy balance. Monolayers were expanded and recompressed at least twice to anneal the sample before transfer to freshly cleaved, hydrophilic mica by vertical deposition with a dipping speed of 5 mm/min.

AFM measurements were carried out on a Multimode Nanoscope III atomic force microscope (Digital Instruments, Santa Barbara, CA) in the repulsive mode in air. The J scanner (120 μm) and 200-μm-long soft cantilevers with integrated pyramidal silicon nitride tips (spring constant of $\sim$60 mN/m) were used for all measurements. Typical scan rates and forces were 1 Hz and 2 nN, respectively. Either duplicate or triplicate samples were prepared for each monolayer composition and at least three separate areas were imaged for each sample. The surface area covered by particular domains was estimated using the bearing analysis routine provided with the DI software.

RESULTS

Isotherms for DPPC, GM1, and DPPC/GM1 monolayers

The surface pressure (π) versus area isotherms for DPPC, GM1, and DPPC/GM1 monolayers at the air/water interface at room temperature (20°C) are shown in Fig. 1 *A*. The isotherm for DPPC shows a characteristic plateau (Tamm and McConnell, 1985) where both LE and LC phases coexist at surface pressures ranging from 6 to 10 mN/m.

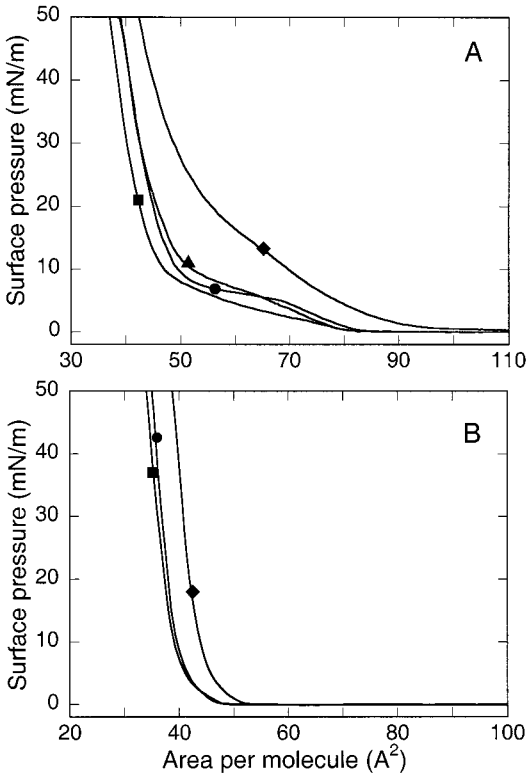

FIGURE 1 Surface pressure versus area/molecule isotherms for DPPC, cholesterol, GM1 and mixtures at the air water interface at room temperature (20°C). (*A*) Isotherms for DPPC (●), GM1 (♦), 2.5% GM1/DPPC (▲), and 10% GM1/DPPC (■). (*B*) Isotherms for 2:1 DPPC/cholesterol (●), 10% GM1 in 2:1 DPPC/cholesterol (♦), and 2% GM1 in 68:30 DPPC/cholesterol (■).

Above 20 mN/m, the DPPC monolayer is in a condensed (solid) phase. The isotherm for a pure GM1 monolayer is expanded by comparison to that for DPPC and shows a phase transition shoulder separating the LE and LC phases, in agreement with previous results (Luckham et al., 1993). Both the large oligosaccharide headgroup and electrostatic interactions due to its negative charge contribute to the expansion of the monolayer. The observed phase transition has been attributed to electrostatic interactions between the charged headgroups rather than the rearrangement of the large polar headgroup (Luckham et al., 1993). The isotherm for 2.5% GM1/DPPC is similar to that for pure DPPC, although the phase transition between the LE and LC phases becomes less well-defined as more GM1 is added. A decrease in the average area/molecule is observed upon addition of 10% GM1. This is consistent with literature results for GM1/DPPC mixed monolayers and has been attributed to complimentary packing interactions between ganglioside and phospholipid molecules (Luckham et al., 1993). The limiting areas for both GM1 and DPPC (~38 and 44 Å^2/molecule, Fig. 1 *A*) are in reasonable agreement with literature results (41 Å^2 for DPPC (Tamm and McConnell, 1985) and 50 Å^2 for GM1 at 26°C, pH 5 (Luckham et al., 1993)), after accounting for variations in temperature and subphase in the different experiments.

AFM images of DPPC/GM1 monolayers

Mixed monolayers of DPPC and GM1 at three different concentrations were transferred to mica at both low (7 mN/m) and high (45 mN/m) surface pressures. These two pressures correspond to regions of mixed LE/LC phases (7 mN/m) and the solid condensed phase for pure DPPC monolayers. Estimates of surface pressures in biological membranes range from 30 to 45 mN/m (Demel et al., 1975; Feng, 1999; Nagle, 1976); a recent detailed study of the use of supported monolayers as models for predicting bilayer properties indicates that higher pressures provide the best comparison (Feng, 1999). AFM images for samples of GM1/DPPC transferred at 7 mN/m are shown in Fig. 2, along with representative examples of a pure DPPC monolayer transferred under similar conditions. The image for DPPC (Fig. 2 *A*) clearly shows the presence of large nearly circular LC domains that are ~10 μm in diameter and ~0.8 nm higher than the surrounding LE phase; a large number of small LC islands are clearly visible in the LE phase. Smaller-scale images (Fig. 2 *B*) for pure DPPC show that the LC phase is quite homogeneous, with a few small LE patches in the large LC domains. These results are in good agreement with previous scanned probe microscopy results for DPPC (Hirai and Takizawa, 1998; Hollars and Dunn, 1997, 1998; Yang et al., 1995), and with ellipsometry (Losche et al., 1984) and fluorescence microscopy experiments (Moy et al., 1986; Rice and McConnell, 1989; Worthman et al., 1997).

Large-scale images of DPPC monolayers containing 2.5, 5, and 10% GM1 are qualitatively similar to those for DPPC alone; large LC domains surrounded by a heterogeneous LE phase containing numerous small LC islands (see Fig. 2, *C* and *D* for 10% GM1) are observed. However, examination of smaller-scale images reveals that the large LC domains are not homogeneous. As shown in Fig. 3 for a sample containing 5% GM1, the centers of the LC domains contain large numbers of brighter dots that are 0.8 nm in height, and there are also larger dots that are 1.2 nm higher than the LC phase scattered along the edge of the large domains (see section analysis, Fig. 3 *C*). By contrast, the smaller LC islands in the surrounding LE matrix are reasonably homogeneous, although brighter dots adjacent to several of the small LC islands can be detected in Fig. 3 *A*. Samples containing 2.5% GM1 (data not shown) are similar to the 5% samples, but with smaller numbers of the higher dots at the edge and in the center of the large LC domains. At higher GM1 concentration (10%) some of the dots on the edges of the LC domains coalesce into fence-like structures, as shown for the large domain in Fig. 2 *E*. Zooming in on a different LC domain shows that the dots in the center have coalesced to give interconnected filaments that are ~1 nm

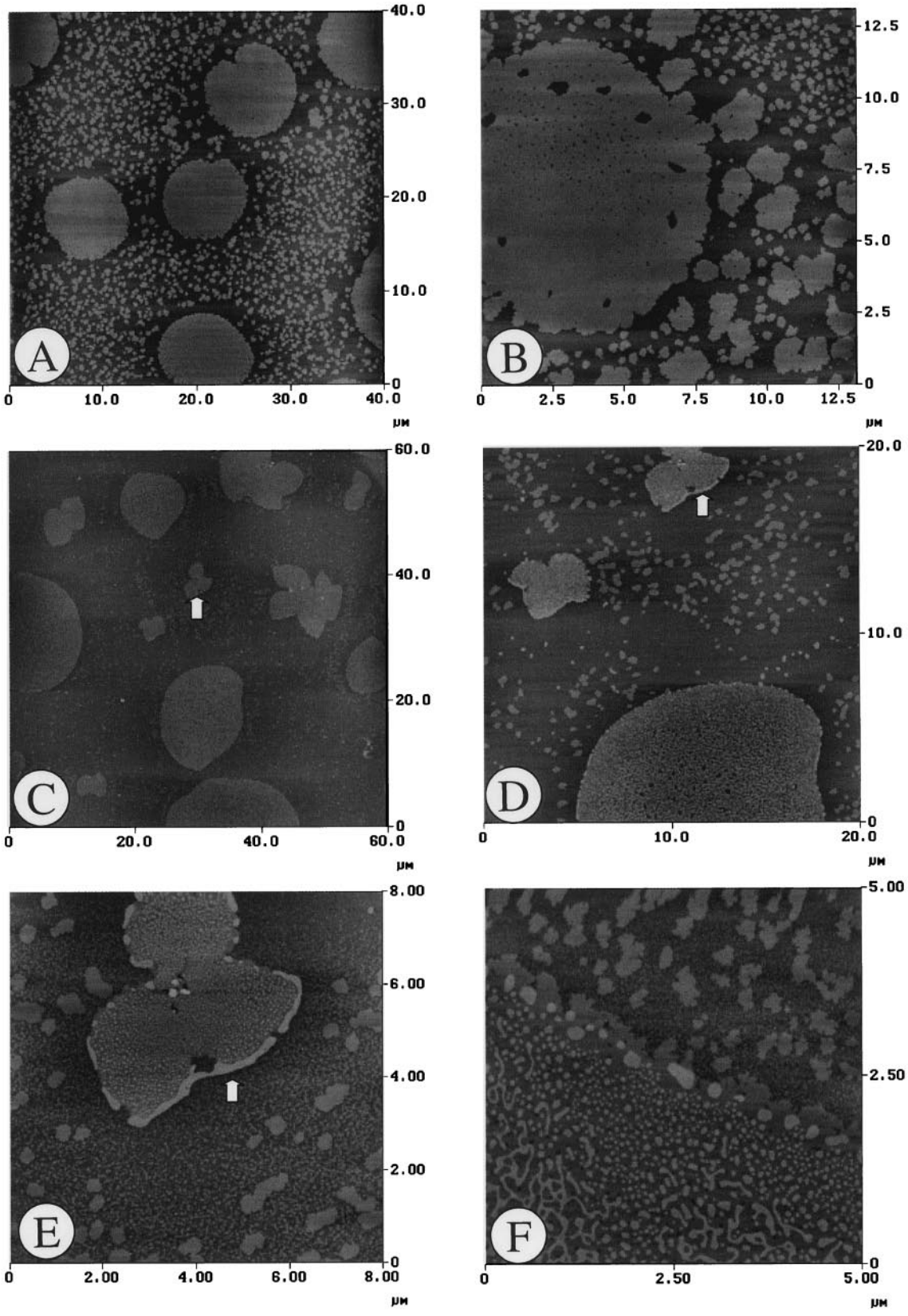

FIGURE 2 AFM images of DPPC (*A*, *B*) and 10% GM1/DPPC monolayers (*C–F*) transferred at 7 mN/m. The *z*-scale is 10 nm for all except *C*, which is 20 nm. Images *D* and *E* were recorded by zooming in on the small domain marked with an arrow in image *C*.

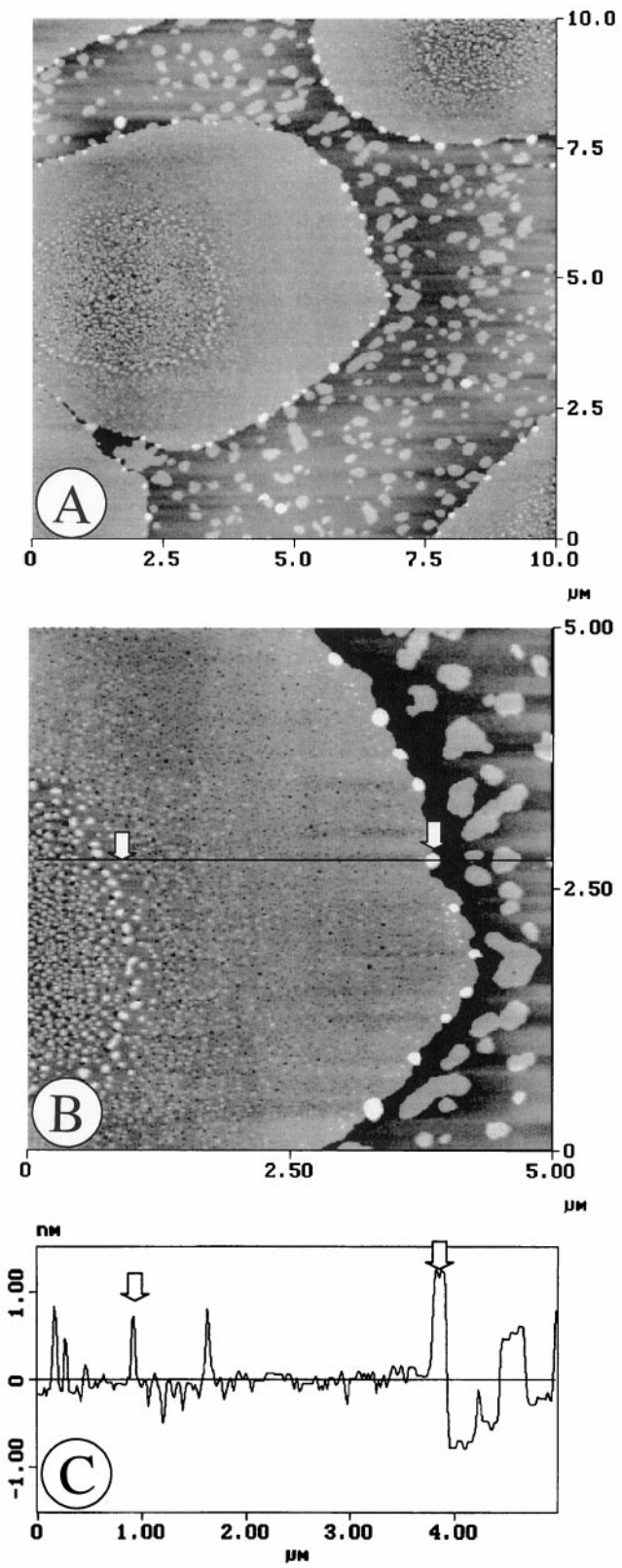

FIGURE 3 AFM images (*A*, *B:* *z*-scale 3 nm) of 5% GM1/DPPC monolayers transferred at 7 mN/m. The section analysis plot (*C*) shows the height differences between the small dots in the middle and at the edge of the large domain and the surrounding LC and LE phases.

higher than the LC phase (Fig. 2 *F*). The larger dots on the edge of the LC domain are ~1.8 nm higher than the surrounding LC matrix, slightly higher than the filaments in the center.

Representative AFM images of DPPC/GM1 monolayers transferred at 45 mN/m are shown in Fig. 4. At this high surface pressure, DPPC monolayers are in the solid (gel) phase and are uniformly flat with occasional small defects (Fig. 4 *A*). By contrast, addition of GM1 again leads to a heterogeneous monolayer, for which a large-scale image shows a pronounced flower-like pattern (10% GM1, Fig. 4 *B*). The interior of the higher flower-like domains contains numerous thin filaments that are ~0.9 nm in height (Fig. 4 *C*, section analysis in 4 *E*). The area surrounding the larger domains is more homogeneous and resembles a pure DPPC monolayer; the difference between the filaments observed within the flower domains and the more homogeneous phase surrounding them is clearly evident in the upper right corner of Fig. 4 *D*. Qualitatively similar results are obtained with 2.5% GM1; large-scale images show evidence for micron-sized domains, although these are less pronounced than those observed for 10% GM1, and small-scale images show the same heterogeneous structure within the large domains. Large round domains are observed for 5% GM1. The area covered by the domains increases with increasing GM1 concentration, although the small height difference and the heterogeneity of the domains make it difficult to obtain quantitative data on these changes.

For comparison purposes, monolayers of pure GM1 were also transferred to mica and imaged under similar conditions to those used for the DPPC/GM1 mixtures. At low surface pressure (7 mN/m) the monolayer is heterogeneous, with a number of irregularly shaped domains (Fig. 5 *A*) that are ~0.5 nm higher than a surrounding heterogeneous phase that has numerous small holes (1.3 nm depth, tens of nanometers in diameter). A small-scale image (Fig. 5, *B* and *F*) shows a network of filaments with some larger dark areas that are clearly the holes observed at larger scan sizes. It is possible to scan rapidly with large force (20 nN/m, 30 Hz scan rate) and create a hole in the monolayer (Fig. 5 *C*). This gives a thickness of ~2.4 nm (Fig. 5 *E*) indicating that the apparent holes in Fig. 5, *A* and *B* are not mica, but contain GM1. At higher surface pressure (45 mN/m) the GM1 monolayer still shows small irregularly shaped brighter domains, although the surrounding phase is much more uniform than at lower pressure (Fig. 5 *D*).

Isotherms for DPPC/cholesterol/GM1 monolayers

The surface pressure versus area isotherms for DPPC/cholesterol and DPPC/cholesterol/GM1 monolayers are shown in Fig. 1 *B*. A 2:1 molar ratio of DPPC/cholesterol was selected because concentrations >~30% cholesterol give a uniform liquid-ordered phase, and this fraction of cholesterol is similar to that found in detergent-insoluble mem-

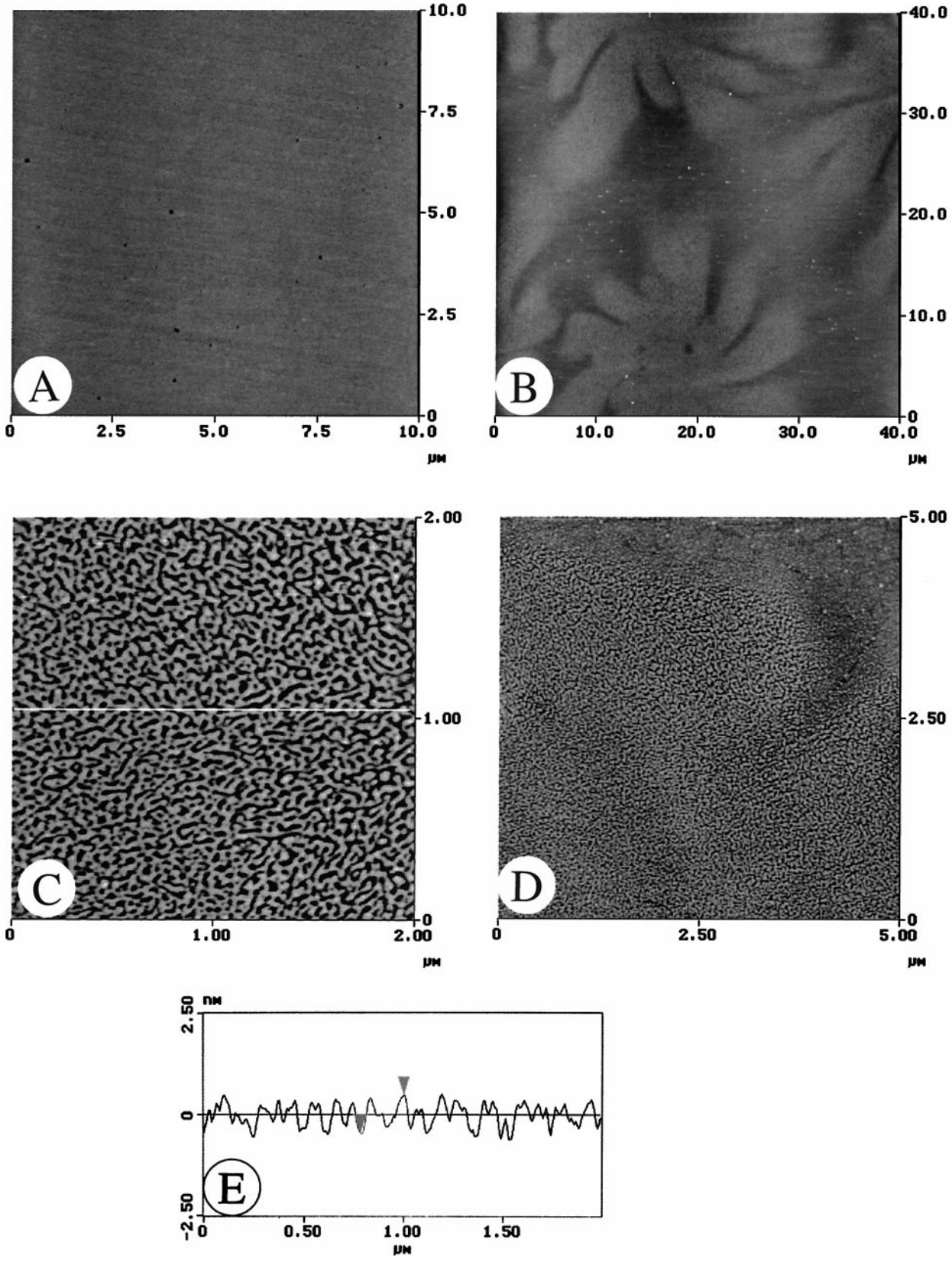

FIGURE 4 AFM images for DPPC (*A*) and 10% GM1/DPPC (*B–D*) monolayers transferred at 45 mN/m. The *z*-scale is either 5 (*A*, *C*, *D*) or 10 nm (*B*). The section analysis is for image (*C*).

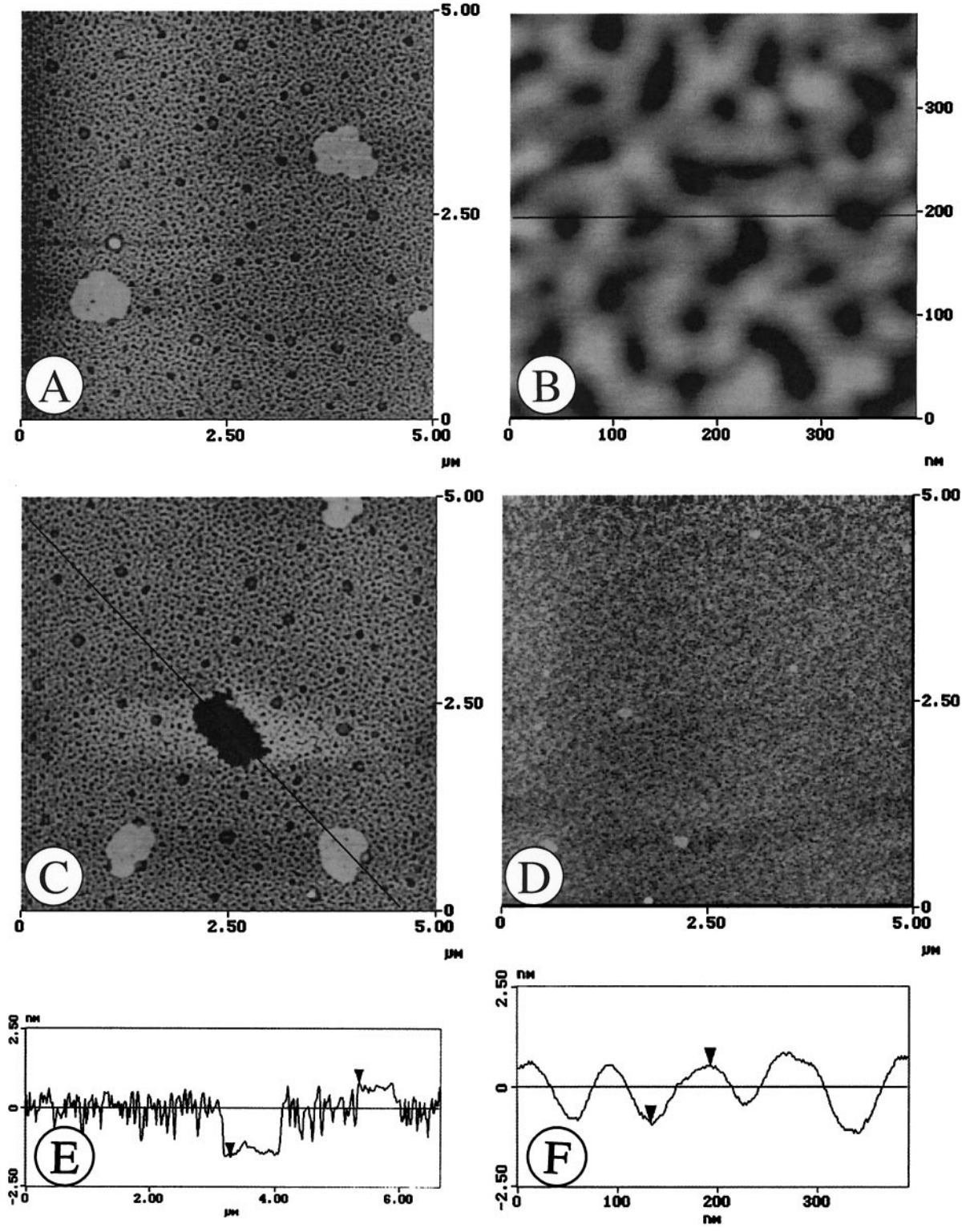

FIGURE 5 AFM images for GM1 monolayers transferred at 7 (*A–C*) or 45 (*D*) mN/m. The *z*-scale is 5 nm for each image. The dark hole in image 2 *C* was produced by rapidly scanning (30 Hz) a 500 nm square at high force (20 nN) with a rapid switch in scan angle from −45 to 135. The switch in scan angle results in a rectangular-shaped hole. The section analysis plots in (*E*) and (*F*) are for images (*C*) and (*D*), respectively.

brane fractions (Brown and London, 1998b; Brown and Rose, 1992; McMullen and McElhaney, 1996). The isotherm for 2:1 DPPC/cholesterol no longer shows the characteristic phase transition between LE and LC phases that is observed for DPPC alone. Rather, the isotherm is shifted to the left, giving a significantly reduced mean area/molecule, and shows a steeply rising slope indicative of a single homogeneous phase. These results are in good agreement with literature data for DPPC/cholesterol mixtures (Worthman et al., 1997). Addition of 2% GM1 leads to only minor changes in the isotherm, whereas the addition of 10% GM1 leads to a slight expansion of the monolayer consistent with the isotherm for GM1 alone shown in Fig. 1 *A*. This is in contrast to the results for DPPC alone, where 10% GM1 leads to a decreased average molecular area.

AFM images of DPPC/cholesterol/GM1 monolayers

AFM images of DPPC/cholesterol (68:30 molar ratio) monolayers containing 2% GM1 and transferred to mica at 7 mN/m and 45 mN/m are shown in Fig. 6. At both pressures the monolayers show a large number of randomly distributed small dots as shown in Fig. 6 *A* for a sample deposited at 7 mN/m. It is important to note that control experiments for DPPC/cholesterol monolayers (2:1 molar ratio) in the absence of GM1 give flat uniform monolayers at both high and low pressures. An example is shown in Fig. 6 *B* for a sample deposited at 7 mN/m. Small-scale images of monolayers containing 2% GM1 show that the domains at low pressure (Fig. 6 *C*) vary in size from 40 to 150 nm. The smallest domains are ~0.7 nm high; the larger ones are ~1.3 nm high at the edges with slightly lower centers, as shown in the section analysis in Fig. 6 *E*. Note that the height variation across the larger domains does not show up well in Fig. 6 *C*, but is clear in the section analysis. At 45 mN/m there are a larger number of smaller domains ($<$50 nm, Fig. 6 *D*) that vary in height from ~0.8 to 1.2 nm (Fig. 6 *F*). Despite the difference in the number and sizes of the small round domains, they account for ~10% of the total area at both pressures.

Images recorded for a similar DPPC/cholesterol (2:1) mixture containing 10% GM1 are shown in Fig. 7. At low surface pressure (7 mN/m) the monolayer shows a uniform network of filaments that are ~1.3 nm higher than the surrounding matrix (Fig. 7 *A*). A small-scale image (Fig. 7 *B*) shows that there are some small hole defects (0.5 nm deep, section analysis, Fig. 7 *E*) in the lower phase of the monolayer. The higher phase covers ~30% of the monolayer surface. Increasing the surface pressure to 15 mN/m and 30 mN/m gives similar images, except that most of the small holes in the lower phase disappear and the filaments become slightly thinner (Fig. 7 *C*). At higher surface pressures the filaments show several different types of larger-scale organization with areas of more and less densely packed filaments (Fig. 7 *D*, 45 mN/m). Comparison of the 10-μm images shown in Fig. 7, *A* and *D* clearly shows this additional longer-range order in the structure of the filament-like domains at high surface pressure. The filaments account for 38% of the surface area for samples deposited at 45 mN/m.

Samples containing 5% GM1 showed a combination of small round domains and longer filaments with step heights of ~1.4 nm at both surface pressures (Fig. 8, *A* and *B*). This suggests that the long filaments form by coalescence of increasing numbers of small round domains as the ganglioside concentration increases. The higher phase accounts for ~13% of the monolayer surface at both surface pressures.

DISCUSSION

The results described above clearly demonstrate that incorporation of biologically relevant concentrations of GM1 in phase-separated DPPC monolayers does not substantially alter the monolayer morphology; both large LC domains and smaller islands in the surrounding LE phase are still observed, as shown in Fig. 2. However, the addition of GM1 leads to significant heterogeneity in the large LC domains. This heterogeneity is manifested by the appearance of small higher dots in the center of the LC domains and additional bright dots at the interface between the LC and LE phases for 2.5 and 5% GM1. With 10% GM1 the small dots in the center of the LC domains coalesce to give numerous longer filaments and the bright patches near the interface of the LC domains become larger and more abundant. The additional microdomains in the LC phase are assigned to GM1-rich areas because their number and size increase with increasing GM1 concentration and the measured height differences are consistent with the differences in length between DPPC and GM1 molecules. In fact, a recent x-ray diffraction study of GM1/phosphatidylcholine bilayers indicates that the ganglioside extends 1.2 nm beyond the lipid headgroup (McIntosh and Simon, 1994). Our results for phase-separated pure DPPC monolayers are also quite similar to literature results for localization of GM1 in the solid DPPC phase of two-component PC monolayers (Vie et al., 1998).

The height of the dots in the center of the large LC domains is consistently less than that of the GM1-rich dots at the interface between the LC and LE phases. These differences may reflect either variable concentrations of GM1 in the microdomains or variations in the length of the GM1 lipid. It is interesting to note that the GM1-induced heterogeneity is confined predominantly to the large LC domains, although there are occasional brighter areas in or adjacent to the small LC islands. This is in contrast to results for 4% GM1 in DOPC/DPPC monolayers for which significant numbers of GM1-rich areas were observed in the small DPPC islands (Vie et al., 1998). It has been argued that the formation of small LC domains in the LE phase of DPPC monolayers transferred at low surface pressures may be

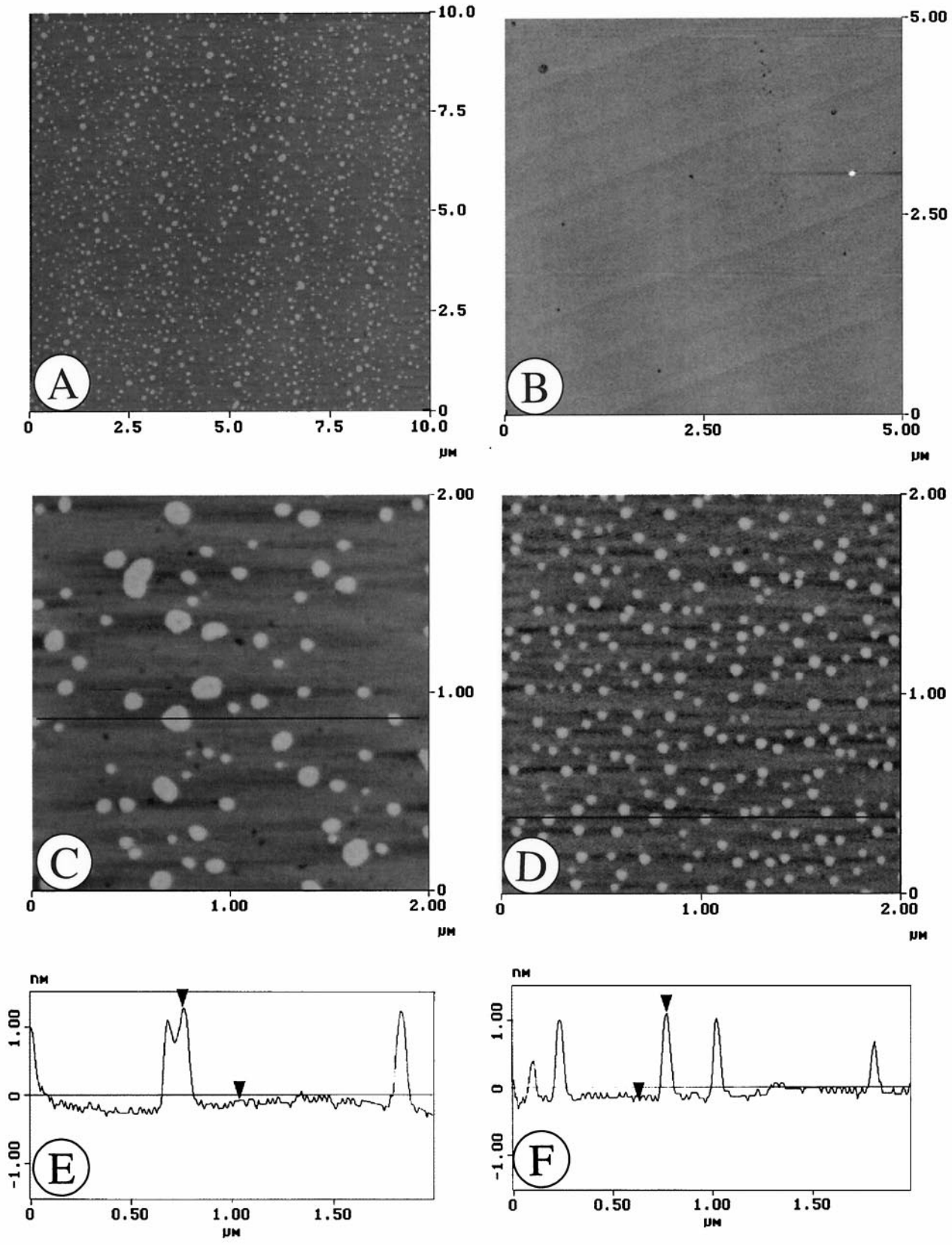

FIGURE 6 AFM images for DPPC/cholesterol (2:1, *B*) and GM1/DPPC/cholesterol (2:68:30, *A*, *C*, *D*) monolayers transferred at 7 mN/m (*A–C*) and 45 mN/m (*D*). The *z*-scales are 10 nm (*A*), 5 nm (*B* and *C*), and 2 nm (*D*).

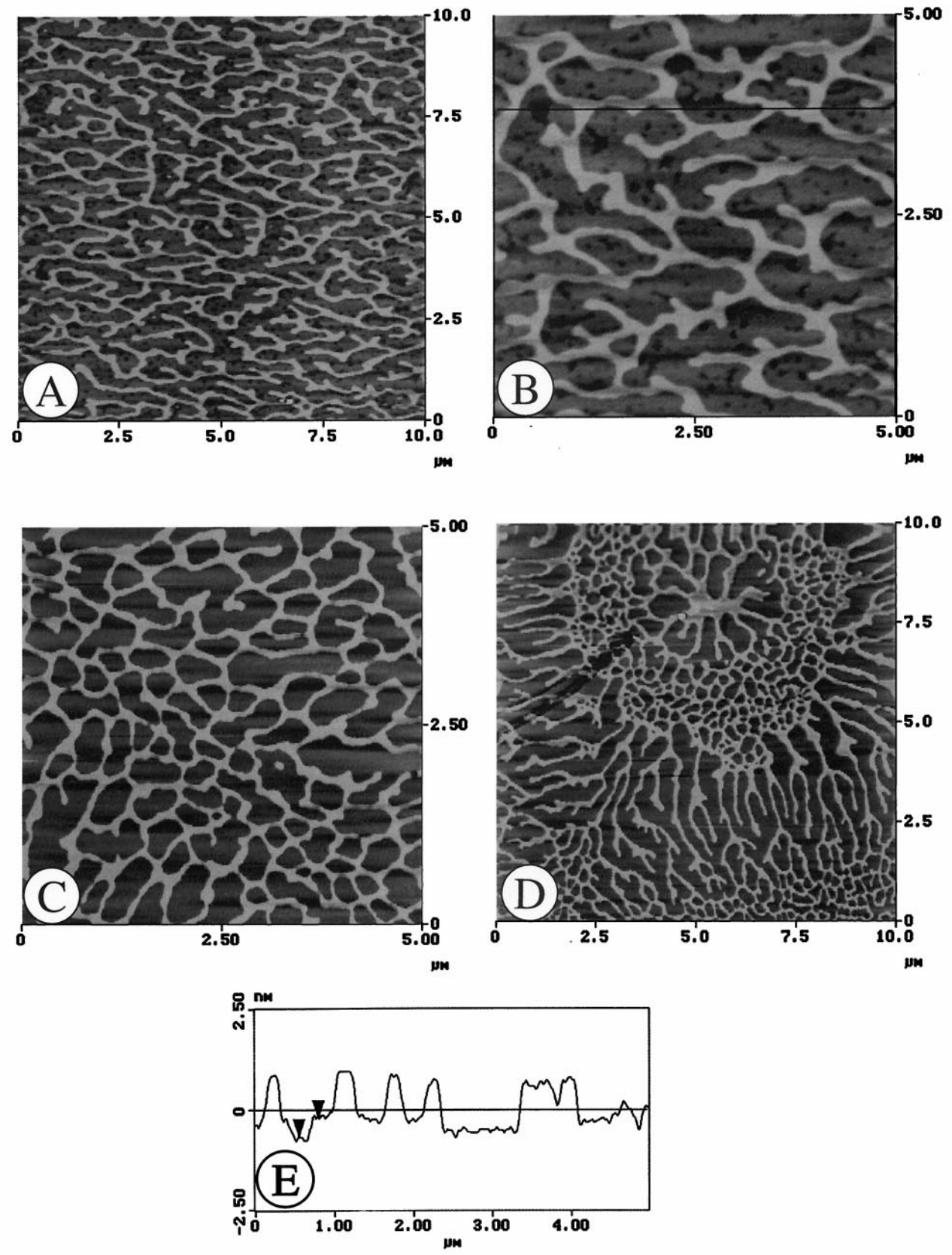

FIGURE 7 AFM images for GM1/DPPC/cholesterol (10:60:30) monolayers transferred at 7 mN/m (*A*, *B*), 30 mN/m (*C*), and 45 mN (*D*). The *z*-scales are 5 nm (*B*) and 10 nm (*A*, *C*, *D*). The section analysis plot (*E*) is for image (*B*).

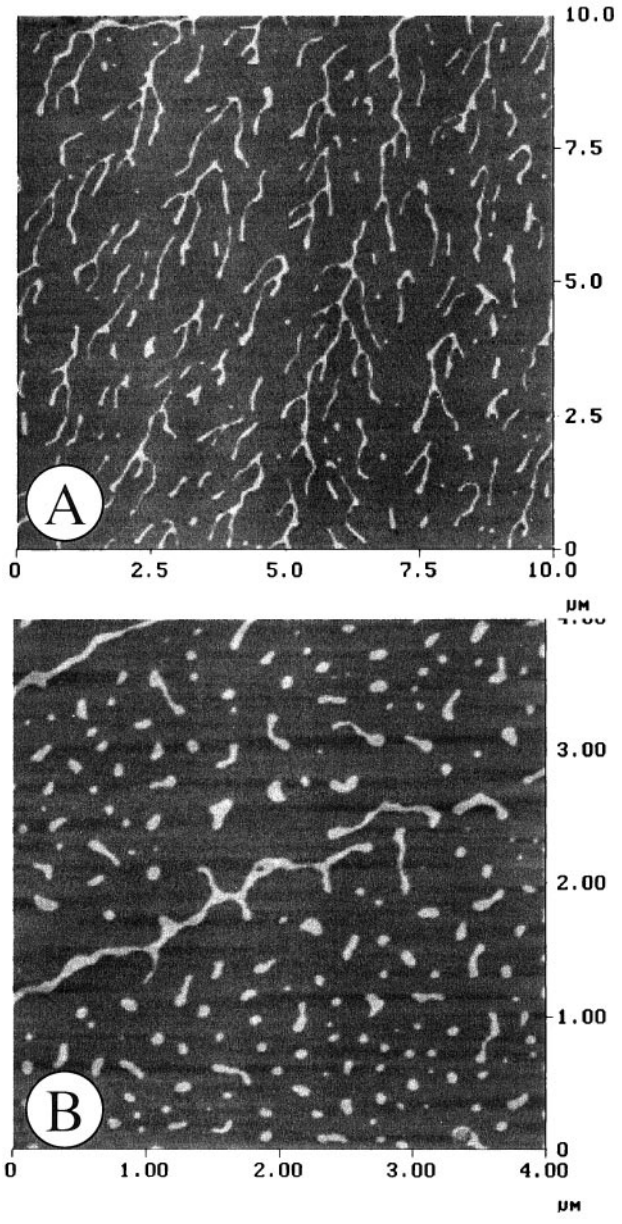

FIGURE 8 AFM images (*z*-scale 10 nm) for GM1/DPPC/cholesterol (5:63.3:31.7) monolayers transferred at 7 mN/m (*A*) and 45 mN/m (*B*).

induced by transfer to the solid support (Shiku and Dunn, 1998).

Significant heterogeneity is observed for GM1/DPPC monolayers transferred at high surface pressure (i.e., corresponding to the solid condensed phase). Although control experiments show that a DPPC monolayer is very flat and uniform under these conditions, the addition of GM1 leads to large circular or flower-shaped domains. The area covered by these structures increases with increasing amounts of GM1 in the monolayer. Furthermore, the domains show heterogeneity on a much smaller scale with the same sort of filamentous network observed for 10% GM1 in the LC domains at low pressure. The combined results at the two pressures clearly demonstrate that GM1 localizes preferentially in the more ordered condensed phase and that its distribution in this phase is heterogeneous under a variety of conditions. Based on the relatively small amounts of GM1 added it is likely that the new microdomains contain both GM1 and DPPC.

As noted above the present results agree well with previous AFM results for two-component monolayers (Vie et al., 1998); the present results remove possible ambiguities due to preferential solubility of GM1 in one of the two lipids or effects of differing hydrocarbon chain lengths (Ferraretto et al., 1997). However, the localization of GM1 in the condensed phase is in contrast to results from a recent near-field scanning optical microscopy study of DPPC monolayers containing 0.5% GM1. Based on fluorescence from a dye that localizes in the more expanded phase of the monolayer, Hwang and co-workers (1995) have concluded that GM1 is trapped in small areas of LE phase that separate the LC domains. The samples used in these experiments had a significantly lower amount of LE phase (due to a higher transfer pressure) than in our studies on the LE/LC monolayers. Furthermore, the concentration of GM1 is lower and the presence of a dye at the same loading may affect the observed monolayer domains. Because the dye used localizes predominantly in the expanded phase, it is unlikely to report on heterogeneity in the condensed phase. A combination of AFM and near-field fluorescence microscopy on the same samples would be required to establish whether the two techniques yield comparable results. Although the AFM and fluorescence experiments appear to sense different domain structures for LE/LC mixtures, it is interesting to note that the web-like structures observed by fluorescence at higher pressure (20 mN/m in the solid condensed phase) (Hwang et al., 1995) are similar to those observed by AFM for the solid condensed DPPC monolayers.

As discussed in the Introduction, previous bilayer studies have come to conflicting conclusions on the preference of gangliosides for localization in liquid crystalline versus gel phases and on their clustering or aggregation in the gel phase. Of particular relevance to our results are studies of GM1 in DPPC/DEPC bilayers, which conclude that GM1 is preferentially located in the gel phase at low concentrations (Rock et al., 1991). Similarly, ESR studies suggest that GM1 is clustered in the gel phase of DPPC bilayers (Delmelle et al., 1980). However, these results are in contrast to AFM studies of supported GM1/PC bilayers (Mou et al., 1995). Incorporation of 10% GM1 was shown to result in a high surface coverage of bound protein when the bilayer was incubated with cholera toxin. The random protein distribution observed for both fluid- and gel-phase PC bilayers provides no evidence for GM1 aggregation. Variations in sample preparation or the fluidity of supported monolayers and bilayers and effects related to protein binding may

contribute to the differences between the monolayer and bilayer results.

DPPC/cholesterol monolayers containing GM1 provide striking evidence for heterogeneity for biologically relevant concentrations of ganglioside. In the absence of ganglioside, 2:1 DPPC/cholesterol mixtures give uniform monolayers that presumably reflect a homogeneous liquid-ordered phase (Brown and London, 1998b; McMullen and McElhaney, 1996) at a variety of surface pressures. Note that this is in contrast to the complex phase behavior of PC/cholesterol mixtures at lower cholesterol concentrations (Rice and McConnell, 1989; Slotte, 1995; Worthman et al., 1997; Yuan and Johnston, manuscript in preparation). Monolayers containing 2% GM1 show numerous small round domains over a wide range of deposition pressures, as illustrated in Fig. 6. Increasing the concentration of GM1 results in a clear evolution to mixtures of small round domains and longer filaments at 5% GM1 and then to a network of interconnected filaments at 10% GM1.

As discussed above for GM1/DPPC mixtures, both the height differences and the increase in the fraction of the new higher phase with increasing ganglioside concentration indicate a GM1-rich phase. From the isotherms at 45 mN/m, one can estimate an area of 44 $Å^2$ for GM1 and an average molecular area of 36 $Å^2$ for the DPPC/cholesterol mixture. The measured amounts of GM1-rich phase of 10, 13, and 38% for 2, 5, and 10% GM1 are significantly higher than would be expected on the basis of the concentrations of GM1 and the limiting molecular areas. Similar conclusions apply at the lower surface pressure, although here the area occupied by a GM1 molecule is substantially higher (74 $Å^2$) than the average for the DPPC/cholesterol mixture (41 $Å^2$). Note that the measured fractions of surface area covered by the new GM1-rich phase may be overestimates in some cases because we have made no attempt to correct for possible tip-convolution effects for the smaller domains. Irrespective of this, it is clear that at both surface pressures the higher domains correspond to a GM1-rich rather than a pure GM1 phase. Electrostatic repulsion between the negatively charged oligosaccharide headgroups of the ganglioside would also be expected to favor a GM1-rich phase over a pure GM1 phase.

The localization of GM1 in the liquid-ordered DPPC/cholesterol monolayer is similar to that observed in the LC domains of DPPC monolayers. In each case there is a clear evolution from small microdomains at low GM1 concentration to a network of filaments at higher concentrations. One important difference is that the small round GM1-rich domains in the 2% GM1 samples are randomly distributed in the PC/cholesterol monolayer, whereas the small dots tend to cluster in the center and at the edges for the LC domains in pure DPPC. The filaments observed for 10% GM1 are also more uniformly distributed in the liquid-ordered monolayer. By contrast to the results for both the liquid-ordered phase and a mixture of LC and LE phases, all concentrations of GM1 examined lead to large domains that contain networks of a GM1-rich phase in solid-condensed DPPC monolayers.

The above-noted similarity between the liquid-ordered and mixed LE/LC monolayers is consistent with the fact that the cholesterol-rich liquid-ordered phase has properties that are intermediate between those of liquid-disordered and gel phases (Brown and London, 1998b; McMullen and McElhaney, 1996). Most literature results (Delmelle et al., 1980; Thompson et al., 1985) indicate that GM1 is randomly distributed in fluid liquid crystalline bilayers, in sharp contrast to its behavior in both gel- and liquid-ordered phases. It is also interesting to note that larger, more heterogeneous microdomains are observed in the liquid-ordered phase (Fig. 6, *C* and *D*), particularly at low surface pressure. This may indicate that initial small domains are mobile and coalesce to give larger heterogeneous domains. Less mobility would be anticipated at higher surface pressure, consistent with the smaller size of the GM1-rich domains in Fig. 6 *D*.

The evolution from circular domains to numerous long interconnected filaments with increasing amounts of GM1 is reminiscent of literature results for cholesterol/phospholipid mixtures at various pressures and compositions (Benvegnu and McConnell, 1993). The variation in domain sizes and shapes has been explained by McConnell and co-workers using a theory based on the competing effects of line tension, which favors circular domains, and long-range dipolar forces that favor extended or striped domains (McConnell, 1991). Similarly, increased dipole-dipole repulsion energy due to the more polar (negatively charged) ganglioside may be responsible for the fact that small GM1-rich aggregates coalesce to give longer filaments rather than larger round domains as the concentration of GM1 is increased. There are also subtle changes in the shape of the LC domains when GM1 is added. This includes some smaller and more irregularly shaped LC domains and the appearance of a smoother interface between the larger LC domains and the surrounding LE phase. This suggests that addition of GM1 changes the balance between line tension and dipolar interactions, even though most of the ganglioside is localized in small microdomains within the LC phase.

Despite the large number of studies that have focused on localization of gangliosides in model bilayers, there is relatively little information on the behavior of ternary PC/cholesterol/ganglioside mixtures. However, the present results can be compared to a recent differential scanning calorimetry investigation of sphingomyelin/cholesterol/GM1 vesicles (Ferraretto et al., 1997), particularly since DPPC and sphingomyelin show similar phase separation behavior (Ahmed et al., 1997). Addition of GM1 to a phase-separated mixture of sphingomyelin/cholesterol led to both GM1-rich and cholesterol-rich phases; GM1 also induced lateral phase separation in sphingomyelin bilayers. The preference for GM1 segregation in sphingomyelin-rich

domains is rationalized on the basis of hydrogen bonding interactions both between gangliosides and between lipids and gangliosides. However, these results are in contrast to the fact that cholesterol, sphingolipids, and glycosphingolipids are enriched in detergent-insoluble membrane fractions. Our AFM results do not provide any means of establishing the relative cholesterol or DPPC concentrations in the GM1-rich domains. Fluorescence microscopy may provide some additional information concerning the relative composition and degree of order in the GM1-rich domains and the surrounding matrix.

The observation of GM1-rich domains in 2:1 DPPC/cholesterol monolayers raises the intriguing possibility that these domains are analogous to lipid rafts. It is particularly interesting that at low ganglioside concentrations one observes small round GM1-rich domains with sizes of ~100 nm within the surrounding liquid-ordered phase. This is in excellent agreement with recent conclusions that glycosylphosphatidylinositol-anchored proteins are localized in submicron domains in living cells (Friedrichson and Kurzchalia, 1998; Varma and Mayor, 1998). The results are also of interest in relation to recent elegant experiments in which phase separation has been detected directly by confocal microscopy in giant unilamellar vesicles composed of DPPC, DLPC, and cholesterol (Korlach et al., 1999) and in which coexistence of lipid domains in binary phospholipid mixtures has been demonstrated (Bagatolli and Gratton, 2000). The ability to directly observe microdomains by AFM measurements on model membranes provides a powerful tool, particularly because such studies are amenable to both force measurements using functionalized tips and to fluorescence microscopy experiments using near-field scanning optical microscopy. Our current experiments aim at using both fluorescence and AFM techniques to examine domain formation in supported bilayers that provide a more realistic membrane model and in more complex mixtures containing both fluid- and liquid-ordered phases.

We thank Dr. D. D. M. Wayner for access to the Nanoscope atomic force microscope.

REFERENCES

Ahmed, S. N., D. A. Brown, and E. London. 1997. On the origin of sphingolipid/cholesterol-rich detergent insoluble cell membranes: physiological concentrations of cholesterol and sphingolipid induce formation of a detergent-insoluble, liquid-ordered lipid phase in model membranes. *Biochemistry.* 36:10944–10953.

Bach, D., I. R. Miller, and B.-A. Sela. 1982. Calorimetric studies on various gangliosides and ganglioside-lipid interactions. *Biochim. Biophys. Acta.* 686:233–239.

Bagatolli, L. A., and E. Gratton. 2000. Two photon fluorescence microscopy of coexisting lipid domains in giant unilamellar vesicles of binary phospholipid mixtures. *Biophys. J.* 78:290–305.

Benvegnu, D. J., and H. M. McConnell. 1993. Surface dipole densities in lipid monolayers. *J. Phys. Chem.* 97:6686–6691.

Brown, D. A., and E. London. 1998a. Functions of lipid rafts in biological membranes. *Annu. Rev. Cell Dev. Biol.* 14:111–136.

Brown, D. A., and E. London. 1998b. Structure and origin of ordered lipid domains in biological membranes. *J. Membr. Biol.* 164:103–114.

Brown, D. A., and J. K. Rose. 1992. Sorting of GPI-anchored proteins to glycolipid-enriched membrane subdomains during transport to apical cell surface. *Cell.* 68:533–544.

Chi, L. F., M. Anders, H. Fuchs, R. R. Johnston, and H. Ringsdorf. 1993. Domain structures in Langmuir-Blodgett films investigated by atomic force microscopy. *Science.* 259:213–216.

Delmelle, M., S. P. Dufrane, R. Brasseur, and J. M. Ruysachaert. 1980. Clustering of gangliosides in phospholipid bilayers. *FEBS Lett.* 121: 11–14.

Demel, R. A., W. S. M. G. Van Kessel, R. F. A. Zwaal, B. Roelofsen, and L. L. M. Van Deenen. 1975. Relation between various phospholipase actions on human red cell membranes and the interfacial phospholipid pressure in monolayers. *Biochim. Biophys. Acta.* 406:97–107.

Derry, D. M., and L. S. Wolfe. 1967. Gangliosides in isolated neutrons and glial cells. *Science.* 158:1450–1452.

Dufrene, Y. F., W. R. Barger, J.-B. D. Green, and G. U. Lee. 1997. Nanometer-scale surface properties of mixed phospholipid monolayers and bilayers. *Langmuir.* 13:4779–4784.

Feng, S.-S. 1999. Interpretation of mechanochemical properties of lipid bilayer vesicles from the equation of state or pressure-area measurement of the monolayer at the air-water interface or oil-water interface. *Langmuir.* 15:998–1010.

Ferraretto, A., M. Pitto, P. Palestini, and M. Masserini. 1997. Lipid domains in the membrane: thermotropic properties of sphingomyelin vesicles containing GM1 ganglioside and cholesterol. *Biochemistry.* 36:9232–9236.

Friedrichson, T., and T. V. Kurzchalia. 1998. Microdomains of GPI-anchored proteins in living cells revealed by crosslinking. *Nature.* 394: 802–805.

Harder, T., P. Scheiffele, P. Verkade, and K. Simons. 1998. Lipid domain structure of the plasma membrane revealed by patching of membrane components. *J. Cell Biol.* 141:929–942.

Hirai, M., and T. Takizawa. 1998. Intensive extrusion and occlusion of water in ganglioside micelles with thermal reversibility. *Biophys. J.* 74:3010–3014.

Hollars, C. W., and R. C. Dunn. 1997. Submicron fluorescence, topology, and compliance measurements of phase-separated lipid monolayers using tapping-mode near-field scanning optical microscopy. *J. Phys. Chem. B.* 101:6313–6317.

Hollars, C. W., and R. C. Dunn. 1998. Submicron structure in L-dipalmitoylphosphatidylcholine monolayers and bilayers probed with confocal, atomic force, and near-field microscopy. *Biophys. J.* 75: 342–353.

Holopainen, J. M., J. Y. A. Lehtonen, and P. K. Kinnunen. 1997. Lipid microdomains in dimyristolyphosphatidylcholine-ceramide liposomes. *Chem. Phys. Lipids.* 88:1–13.

Hwang, J., L. K. Tamm, C. Bohm, T. S. Ramalingam, E. Betzig, and M. Edidin. 1995. Nanoscale complexity of phospholipid monolayers investigated by near-field scanning optical microscopy. *Science.* 270: 610–613.

Jacobson, K., and C. Dietrich. 1999. Looking at lipid rafts? *Cell Biol.* 9:87–91.

Korlach, J., P. Schwille, W. W. Webb, and G. W. Feigenson. 1999. Characterization of lipid bilayer phases by confocal microscopy and fluorescence correlation spectroscopy. *Proc. Natl. Acad. Sci. USA.* 96: 8461–8466.

Losche, M., J. Rabe, A. Fischer, B. U. Rucha, W. Knoll, and H. Mohwald. 1984. Microscopically observed preparation of Langmuir-Blodgett films. *Thin Solid Films.* 117:269–280.

Luckham, P., J. Wood, S. Froggatt, and R. Swart. 1993. The surface properties of gangliosides. *J. Colloid Interface Sci.* 156:164–172.

McConnell, H. M. 1991. Structures and transitions in lipid monolayers at the air-water interface. *Annu. Rev. Phys. Chem.* 42:171–195.

McIntosh, T., and S. A. Simon. 1994. Long- and short-range interactions between phospholipid/ganglioside GM1 bilayers. *Biochemistry*. 33: 10477–10486.

McMullen, T. P. W., and R. N. McElhaney. 1996. Physical studies of cholesterol-phospholipid interactions. *Curr. Opin. Colloid Interface Sci.* 1:83–90.

Mehlhorn, I. E., G. Parraga, K. R. Barber, and C. W. M. Grant. 1986. Visualization of domains in rigid ganglioside/phosphatidylcholine bilayers. *Biochim. Biophys. Acta.* 863:139–155.

Mou, J., J. Yang, and Z. Shao. 1995. Atomic force microscopy of cholera toxin B-oligomers bound to bilayers of biologically relevant lipids. *J. Mol. Biol.* 248:507–512.

Moy, V. T., D. J. Keller, H. E. Gaub, and H. M. McConnell. 1986. Long-range molecular orientational order in monolayer solid domains of phospholipids. *J. Phys. Chem.* 90:3198–3202.

Nagle, J. F. 1976. Theory of monolayer and bilayer phase transitions: effect of headgroup interactions. *J. Membr. Biol.* 27:233.

Overney, R. M., E. Meyer, J. Frommer, D. Brodbeck, R. Luthi, L. Howald, H.-J. Guntherodt, M. Fujihira, H. Takano, and Y. Gotoh. 1992. Friction measurements on phase separated thin films with a modified atomic force microscope. *Nature.* 359:133–134.

Peters, M. W., and C. W. M. Grant. 1984. Freeze-etch study of an unmodified lectin interacting with its receptor in model membranes. *Biochim. Biophys. Acta.* 775:272–282.

Peters, M. W., I. E. Mehlhorn, K. R. Baber, and C. W. M. Grant. 1984. Evidence of a distribution difference between two gangliosides in bilayer membranes. *Biochim. Biophys. Acta.* 778:419–428.

Rice, P. A., and H. M. McConnell. 1989. Critical shape transitions of monolayer lipid domains. *Proc. Natl. Acad. Sci. USA.* 86:6445–6448.

Rinia, H. A., R. A. Demel, J. P. J. M. van der Eerden, and B. de Krujiff. 1999. Blistering of Langmuir-Blodgett bilayers containing anionic phospholipids as observed by atomic force microscopy. *Biophys. J.* 77: 1683–1693.

Rock, P., M. Allietta, W. W. J. Young, T. E. Thompson, and T. W. Tillack. 1991. Ganglioside GM1 and Asialio-GM1 at low concentration are preferentially incorporated into the gel phase in two-component, two-phase phosphatidylcholine bilayers. *Biochemistry*. 30:19–25.

Sharom, F. J., and C. W. M. Grant. 1978. A model for ganglioside behavior in cell membranes. *Biochim. Biophys. Acta.* 507:280–293.

Shiku, H., and R. C. Dunn. 1998. Direct observation of DPPC phase domain motion on mica surfaces under conditions of high relative humidity. *J. Phys. Chem.* 102:3791–3797.

Simons, K., and E. Ikonen. 1997. Functional rafts in cell membranes. *Nature.* 387:569–572.

Slotte, J. P. 1995. Lateral domain formation in mixed monolayers containing cholesterol and dipalmitoylphosphatidylcholine or N-palmitoylsphingomyelin. *Biochim. Biophys. Acta.* 1235:419–427.

Tamm, L. K., and H. M. McConnell. 1985. Supported phospholipid bilayers. *Biophys. J.* 47:105–113.

Terzaghi, A., G. Tettamanti, and M. Masserini. 1993. Interaction of glycosphingolipids and glycoproteins: thermotropic properties of model membranes containing GMI ganglioside and glycophorin. *Biochemistry*. 32:9722–9725.

Thompson, T. E., M. Allietta, R. E. Brown, M. L. Johnston, and T. W. Tillack. 1985. Organization of ganglioside GM1 in phosphatidylcholine bilayers. *Biochim. Biophys. Acta.* 817:229–237.

Varma, R., and S. Mayor. 1998. GPI-anchored proteins are organized in submicron domains at the cell surface. *Nature.* 394:798–801.

Vie, V., N. V. Mau, E. Lesniewska, J. P. Goudonnet, F. Heitz, and C. L. Grimellec. 1998. Distribution of ganglioside GM1 between two-component, two-phase phosphatidylcholine monolayers. *Langmuir.* 14: 4574–4583.

Worthman, L.-A. D., K. Nag, P. J. Davis, and K. M. W. Keough. 1997. Cholesterol in condensed and fluid phosphatidylcholine monolayers studied by epifluorescence microscopy. *Biophys. J.* 72:2569–2580.

Yang, X. M., D. Xiao, Z. H. Lu, and Y. Wei. 1995. Structural investigation of Langmuir-Blodgett monolayers of L-α-dipalmitoylphosphatidylcholine by atomic force microscopy. *Appl. Surf. Sci.* 90:175–183.